

# A Preliminary Investigation of an Electrodynamic Wheel for Simultaneously Creating Levitation and Propulsion

J. Bird, T.A. Lipo  
University of Wisconsin-Madison  
1415 Engineering Drive  
Madison, WI, 53706-1691  
jbird@cae.wisc.edu, lipo@engr.wisc.edu

## Keywords

Electrodynamic levitation, Electrodynamic propulsion, Halbach array, Maglev.

## Abstract

The mechanical rotation of a radially positioned permanent magnet Halbach array above a conducting, non-magnetic, track creates a traveling time-varying magnetic field that can inductively create levitation and propulsion forces simultaneously. This ‘Electrodynamic Wheel’ (EDW), could be used to create a relatively cheap form of maglev transportation since the track would not need to be electrified and both the levitation and propulsion forces would be created by one mechanism. The various parameters that influence the performance of such a maglev system have been studied by using a 2D steady-state Finite Element Method. The effect of the pole number, magnet thickness, radius, track thickness, and track conductivity on the EDW performance were considered. Design guidelines and methods to further improve the EDW performance are suggested.

## 1 Introduction

In the 1970’s it was proposed that rotating superconducting magnets over a conductive non-magnetic track could provide an integrated levitation and propulsion mechanism for high-speed ground transportation [1-3]. The rotation of the magnetic sources over a track will enable the drag force, inherent in almost all other maglev systems, to be used as a propulsion force [4]. The propulsion forces are dependent on the relative velocity of the rotor compared to the traveling velocity, and therefore as with linear and rotary induction motors there is a slip. Large breaking forces result when the peripheral velocity of the rotor is spun slower than the vehicle’s traveling velocity. Although it was claimed that the EDW used significantly less energy than other maglev systems [2] further study was not undertaken on the EDW; this was almost certainly in part due to the complexity of needing to rotate helium-cooled superconductors.

With the rapid improvement in rare-earth magnets, it was thought possible to consider using rare-earth magnets rather than superconductors in order to create a low cost EDW with a small air-gap [4]. A number of researchers have been considering using rare-earth magnets for maglev applications. Most recently, Fujii showed that the rotation of axially placed rare-earth permanent magnets over the edge of a conductive track could create lift and propulsion force simultaneously, in addition, guidance forces were created when the track had an incline [5, 6]. Unfortunately the performance when operating with translational motion and thrust efficiency results have not been published, also no scaling discussion has been provided for the axial magnet rotation maglev system. Several authors have proposed that linear Halbach arrays can provide a low cost means of providing sufficient lift force for a maglev system [7, 8]. But using such a system will create a drag force and a separate costly linear synchronous motor is required to create the thrust.

It is the purpose of this paper to study the performance attainable using radial positioned Halbach magnets, rather than axial magnets. Using radial positioned magnets may have an advantage over axial positioned magnets because it should be possible to design a flat guidance track structure using radial magnets, and this would therefore make the track construction costs lower [9]. A discussion on how the pole number, magnet thickness, outer radius, track thickness, and track conductivity influence the performance of the EDW, based on a 2D analysis is presented. Lastly, suggestions for further design improvements will be presented.

The EDW is similar to a linear induction machine (LIM) in that a traveling magnetic field is created and only a passive track is required to create the propulsion. However, unlike the LIM, back iron is not required on the track, thus allowing the normal force to be used to create levitation. Additionally, there are no low power factor problems and the machine can be made relatively light weight.

## 2 The Electrodynamic Wheel Model

The quasi-static electromagnetic field equations when moving conductors are present are:

$$\nabla \times \mathbf{H} = \mathbf{J} = \sigma(\mathbf{E} + v \times \mathbf{B}) + \mathbf{J}_s \quad (1)$$

$$\nabla \times \mathbf{E} = -\frac{\partial \mathbf{B}}{\partial t} \quad (2)$$

$$\nabla \cdot \mathbf{B} = 0 \quad (3)$$

$$\nabla \cdot \mathbf{J} = 0 \quad (4)$$

Where  $\mathbf{H}$  is the magnetic field intensity,  $\mathbf{B}$  is the flux density,  $\mathbf{J}_s$  is an external excitation current source,  $\mathbf{E}$  is the electric field intensity and  $v$  is the relative traveling velocity of the conductive material. Using the definitions of the magnetic vector potential,  $\mathbf{A}$ :

$$\mathbf{B} = \nabla \times \mathbf{A} \quad (5)$$

$$\mathbf{E} = -\frac{d\mathbf{A}}{dt} - \nabla V \quad (6)$$

and the generalized constitutive relation,  $\mathbf{B} = \mu(\mathbf{H} + \mathbf{M})$ , where  $\mathbf{M}$  is the magnetization vector,

(1) may be rewritten as:

$$\sigma \frac{\partial \mathbf{A}}{\partial t} + \nabla \times (\mu^{-1} \nabla \times \mathbf{A} - \mathbf{M}) - \sigma v \times (\nabla \times \mathbf{A}) + \sigma \nabla V = \mathbf{J}_s \quad (7)$$

Also, from (4) we get:

$$-\nabla \cdot \left( \sigma \frac{\partial \mathbf{A}}{\partial t} - \sigma v \times (\nabla \times \mathbf{A}) + \sigma \nabla V - \mathbf{J}_s \right) = 0 \quad (8)$$

Using the Coulomb gauge,  $\nabla \cdot \mathbf{A} = 0$ , and the following identity:  $\nabla \times (\nabla \times \mathbf{A}) = \nabla \cdot (\nabla \cdot \mathbf{A}) - \nabla^2 \mathbf{A}$  and assuming  $\mu$  is constant in the conducting region, (7) can be simplified to:

$$\sigma \frac{\partial \mathbf{A}}{\partial t} + \frac{1}{\mu} \nabla^2 \mathbf{A} - \nabla \times \mathbf{M} - \sigma v \times (\nabla \times \mathbf{A}) + \sigma \nabla V = \mathbf{J}_s \quad (9)$$

For 2D problems where the track is a conducting sheet and  $\mathbf{J}$  is perpendicular to the 2D plane, the scalar potential term,  $V$ , is zero [10]. For computational simplicity the EDW is assumed to be stationary and the track is assumed to move with a constant velocity in the horizontal, x-direction, only. For this 2D analysis the vector potential has only one component,  $A_z$ , which is directed into the page. The second to last term on the left of (9) then simplifies to:

$$\sigma v_x \times (\nabla \times A_z) = -\sigma v_x \frac{\partial A_z}{\partial x} \quad (10)$$

Equation (9) then becomes:

$$\nabla^2 A_z + \mu\sigma \left( \frac{\partial A_z}{\partial t} - v_x \frac{\partial A_z}{\partial x} \right) = J_s + \nabla \times \mathbf{M} \quad (11)$$

For the track region, where there are no magnet or current sources we have:

$$\nabla^2 A_z + \mu\sigma \frac{\partial A_z}{\partial t} + \mu\sigma v_x \frac{\partial A_z}{\partial x} = 0 \quad (12)$$

While in the air,  $\sigma=0$ , and we have:

$$\nabla^2 A_z = 0 \quad (13)$$

For the magnet region:

$$\nabla^2 A_z = \nabla \times \mathbf{M} \quad (14)$$

The track air and magnet regions are thus fully defined by (12)-(14). The circular geometry of the EDW combined with the linear geometry of the track makes solving (12)-(14) analytically a formidable problem and therefore the Finite Element Method has been used. Solving (12)-(14) transiently with both rotational and translational motion at high traveling velocities is also a daunting task. Therefore, in order to model the EDW the Halbach magnets have been replaced with an equivalent complex current sheet,  $J_s$ . Thus (14) becomes:

$$\nabla^2 A_z = J_s e^{jP\theta} \quad (15)$$

along the rotor edge. Where  $P$  is the number of pole pairs and  $\theta$  is the angular position around the rotor edge. The magnitude of the fictitious current sheet,  $J_s$ , has been made to match the magnetic vector potential value around the Halbach magnet rotor edge. Fortunately, for the Halbach rotor the magnetic vector potential is almost exactly sinusoidal. An illustration of the vector potential field lines for a 4 pole-pair Halbach rotor and an equivalent current sheet rotor is shown in Figures 1 and 2 respectively.

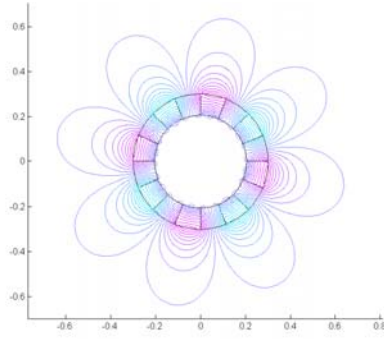


**Fig. 1 Magnetic Field for Halbach Rotor**

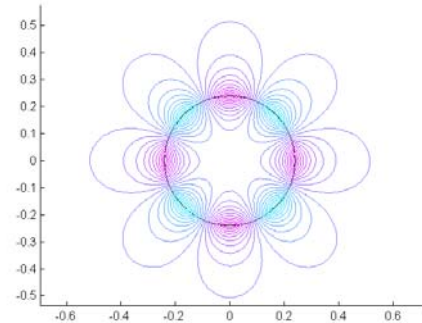


**Fig. 2 An Equivalent Current Sheet Rotor**

The use of the equivalent fictitious complex current-sheet enables the magnets rotational motion to be modeled using complex steady-state FEA methods and therefore no transient finite element rotating air-gap method is required. The time derivative term in (12) then becomes simply  $j\omega A_z$ . The use of the equivalent current sheet neglects any losses that occur within the magnets. The formulation of the EDW model was created in FEMLAB which runs within Matlab and therefore allows a full parameter analysis to be programmed. The current sheet steady-state models developed in FEMLAB were validated by comparing the results from Magsoft Flux 2D transient models using a Halbach rotor with no horizontal motion. Also comparisons were made with Magsoft for the case of transient translational motion with no rotating air-gap. In both these rotational and translational transient simulations the steady-state model gave equivalent results.

An illustration of the field lines created for a 6 pole-pair EDW model rotating at 4700rpm and traveling at 80 m/s over a 10mm thick aluminum track is shown in Figure 3. Figure 4 and 5 shows

how the propulsion and levitation forces change when the slip and traveling velocity are varied. Where slip,  $s = \omega r - v$  and  $\omega$  is the angular velocity and  $r$  is the rotor radius. All the parameters used to produce Figures 4 and 5 are shown in Table 1.

The lowering of the thrust force at high velocity shown in Figure 4 is mainly due to the vertical component of rotor flux being prevented from interacting with the induced track currents due to the large opposing magnetic field in the track, which gives rise to the levitation force. Figure 5 shows that large levitation forces can be created at all slip values when the traveling velocity becomes relatively high.

### 3 Determining the Optimal Magnet Thickness and Pole Number

#### 3.1 Optimal Halbach Rotor Thickness

The Halbach magnet rotor thickness was determined by finding the optimal rotor thickness for each pole number that minimized the mass divided by flux squared performance index [11]:

$$F = \frac{\text{mass}}{\text{flux}^2} \quad (16)$$

Minimizing this performance index gives the optimal magnet thickness that gives the highest lift-to-weight ratio. The flux was computed across the surface of the track directly below the rotor. The inner-to-outer rotor radius ratio is defined as:

$$t = \frac{r_{in}}{r_{out}} \quad (17)$$

It was determined that the optimal ratio, for the inner-to-outer radius for each pole-pair did not depend on the outer radius value.

The confirmation that minimizing (16) gives the optimal lift-to-weight ratio was achieved by running an EDW force analysis for a range of Halbach rotor magnet thicknesses. When (17) was varied, it was determined that the maximum lift-to-weight ratio for a 7 pole-pair rotor was achieved when  $t=0.82$ , as shown in Figure 6. Whereas minimizing (16) also gave the same ratio for the 7 pole-pairs case. The optimal inner-to-outer rotor radius ratio for 2 to 7 pole-pairs is shown in Figure 7. The increase in this ratio with the number of pole-pairs results in a decreasing rotor mass with pole number, as shown in Figure 8.

**Table 1.**

Travel velocity	Varied
Slip	Varied
Outer radius	0.23m
Track conductivity	3.5e7
Track thickness	10mm
Magnet width	0.15m
Air gap	10mm
Pole pairs	6
Residual Magnetization (N50m), $B_r$	1.42T

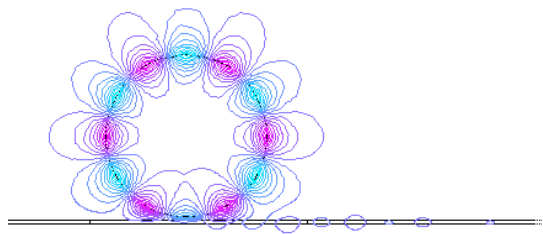


**Fig. 3 A Six Pole Pair Electrodynamic Wheel**

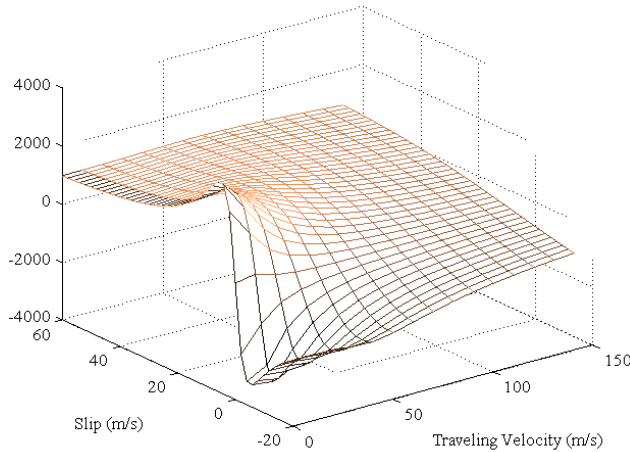


**Fig. 4. Thrust vs. Slip and Travel Velocity**

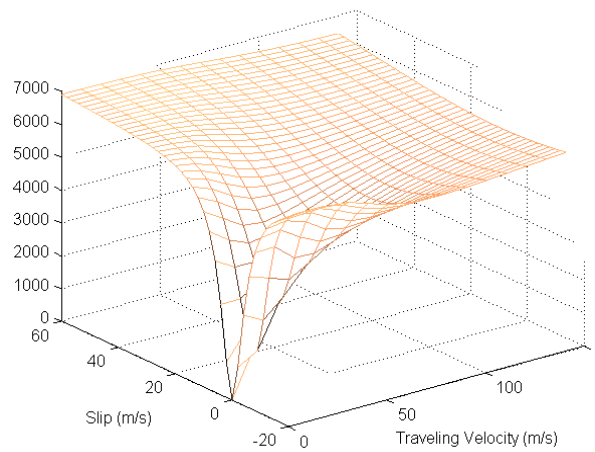


**Fig. 5 Lift Force vs. Slip and Travel Velocity**

### 3.2 The Influence of Pole Number on Performance

The parameters used for the pole-pair analysis are the same as in Table 1, except the traveling velocity and slip have been set at 135m/s and 45m/s respectively. The slip and traveling velocity have a significant effect on the performance of the EDW but the general relationship between the pole number and the performance measures are independent of the slip and travel velocity. Therefore, 2D curves have been used to show the relationships. Figure 9 illustrates the lift-to-weight ratio achievable for the given parameters. A pole-pair number of 4 gives the highest lift-to-weight ratio, and this is true thorough-out the slip range. Figure 10 shows that the levitation force decreases as the pole number increases, whilst Figure 11 shows that the thrust force plateaus after 6 pole pairs. The levitation force, shown in Figure 10, monotonically decreases at higher pole numbers because the flux magnitude using higher poles decreases at the track surface for the same air gap. The power requirements are shown in Figure 12. Figure 13 shows that the thrust efficiency increases with increasing pole number. This is because at higher pole numbers the electrical frequency becomes higher and this allows the flux to penetrate further into the track, when traveling at high velocities, before sufficient current has been induced to fully create an opposing field. The result is that the track power loss decreases with increasing pole number at a faster rate compared with the thrust.

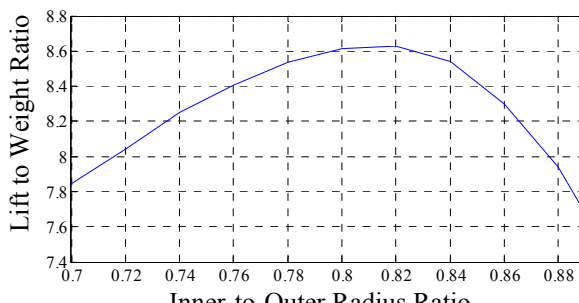


**Fig. 6 Confirming Optimal Lift to Weight Ratio for 7pp Case**

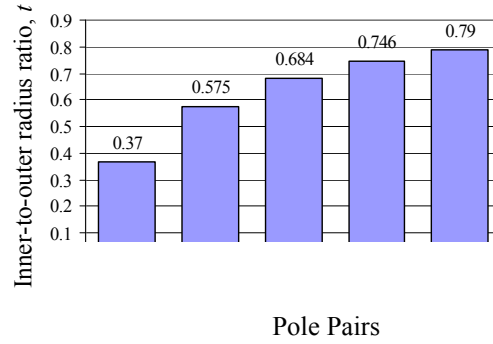


**Fig. 7 Optimal Inner-to-Outer Radius Ratio vs. Pole No.**

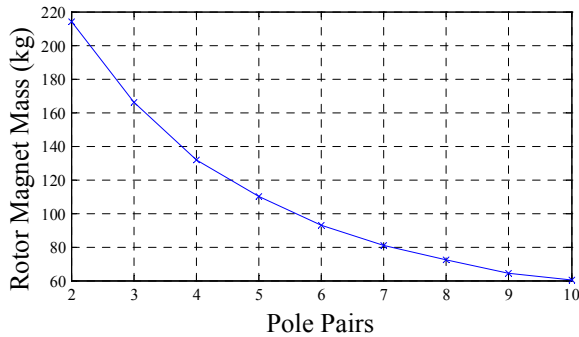


**Fig. 8 Rotor Magnet Mass vs. Pole Number**

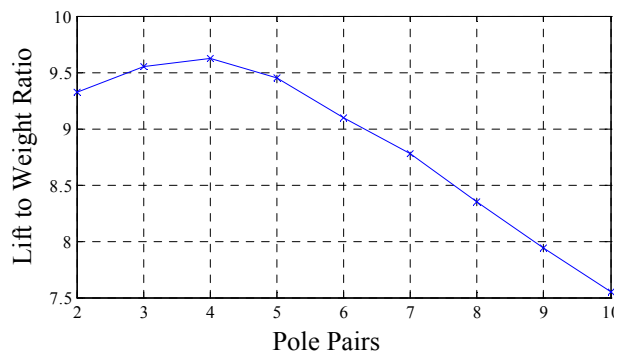


**Fig. 9 Lift-to-Weight Ratio vs. Pole Number**

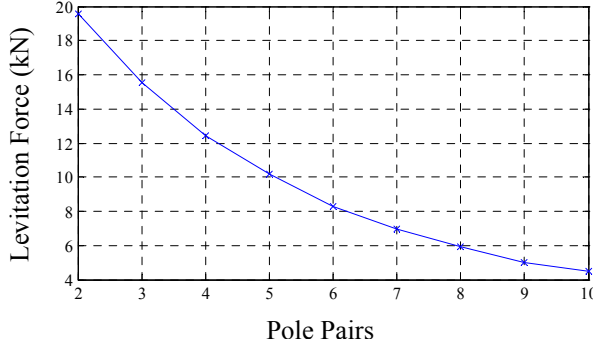


**Fig. 10 Levitation Force vs. Pole Number**

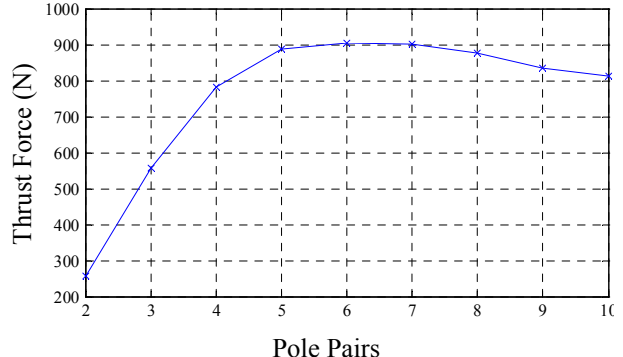


**Fig. 11 Thrust Force vs. Pole Number**

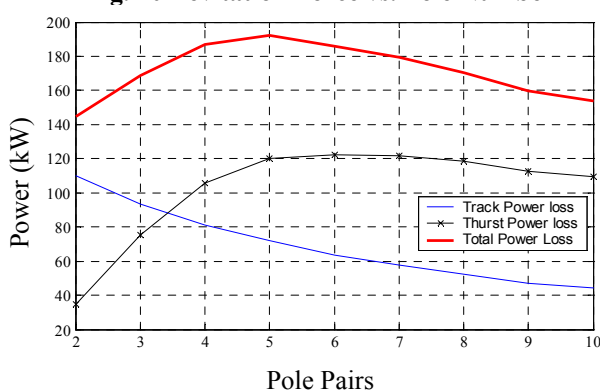


**Fig. 12 Track and Thrust Power vs. Pole No.**

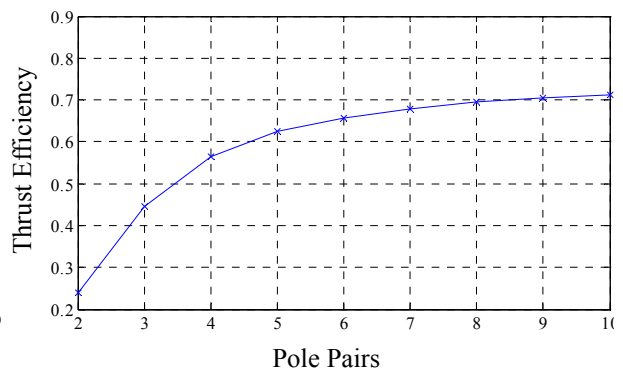


**Fig. 13 Thrust Efficiency**

Although the thrust efficiency can be higher for a linear synchronous motor maglev system, it must be remembered that no additional system or energy is needed to also create the lift force for the EDW.

### 3.3 The Influence of Rotor Radius on Performance

As the outer radius increases the thrust and lift forces increase linearly, as illustrated in Figure 14 and 15. The forces are proportional to the track area, therefore as the rotor radius increases the area and hence total flux increases thereby giving a linear increase in force. However, the rotor mass increases proportionally to the square of the radius, as shown in Figure 16, and therefore this leads to a linearly decreasing lift-to-weight-ratio with radius, Figure 17. At very low radii the flux along the track at the given air-gap becomes very weak and this causes the reduction in the lift-to-weight ratio below 0.15m. This reduction in the lift-to-weight ratio at small radii becomes severe above 6 pole-pairs.

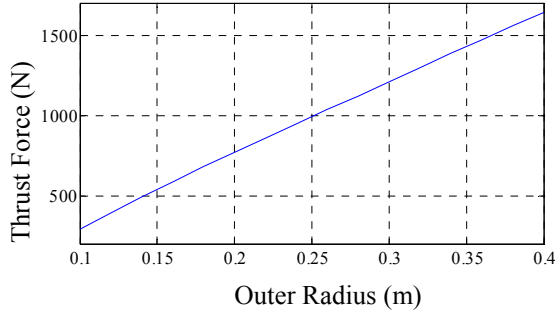


Fig. 14 Thrust Force vs. Outer Radius

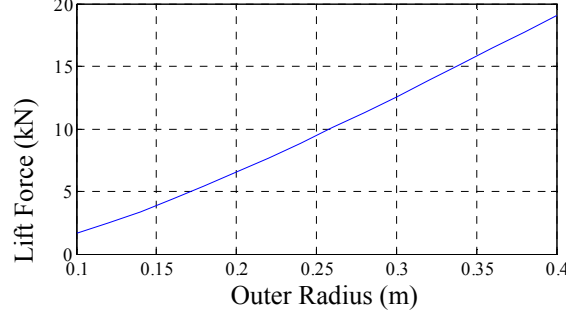


Fig. 15. Lift Force vs. Outer Radius

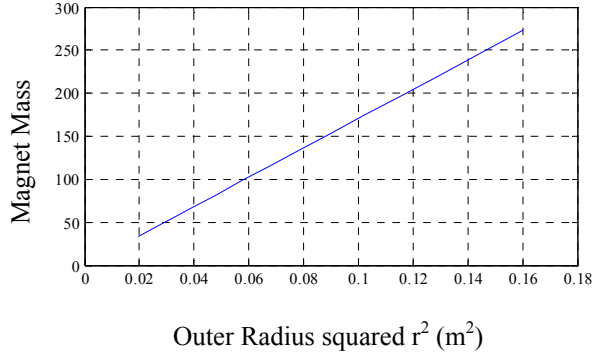


Fig. 16 Magnet Mass vs. Outer Radius Squared

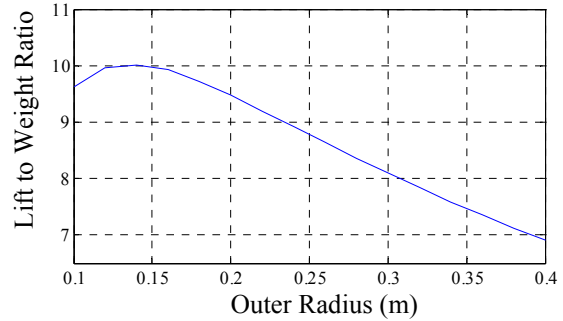
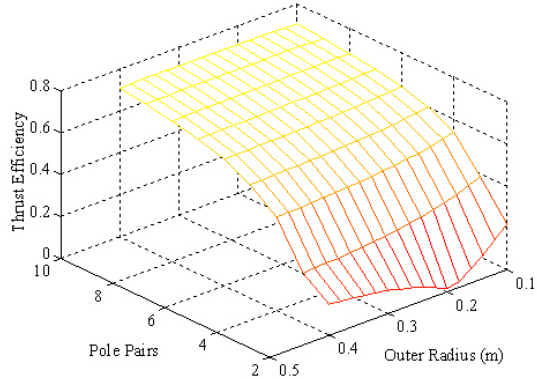


Fig. 17 Lift-to-Weight Ratio vs. Outer Radius

### 3.4 Rotor Radius vs. Pole Pairs

The ability to continually increase the thrust efficiency by increasing the number of poles is limited by the strength of the magnets since at higher pole numbers the amount of flux penetrating the track diminishes for a given air-gap and results in a diminishing lift-to-weight ratio. The trade-off between the pole number and outer radii on the lift-to-weight-ratio and thrust efficiency is illustrated in Figure 18 and 19. The parameters used to generate these two plots are the same as used previously. Figure 18 interestingly shows that as the pole number increases the effect of the radius on the thrust efficiency becomes negligible, at 10 pole-pairs the change in thrust efficiency is just 1% over the range of radii plotted. Figure 19 clearly shows the reduction in the lift-to-weight ratio when the number of pole-pairs and outer radius increases.



**Fig. 18 Thrust Efficiency vs. Outer Radius and Pole-Pairs**

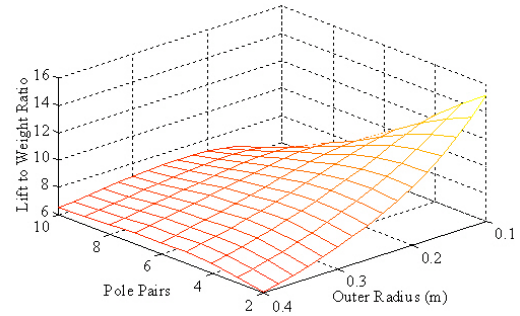


**Fig. 19 Lift to Weight Ratio vs. Pole-Pairs and Outer Radius**

### 3.5 Track Thickness and Track Conductivity

Increasing the track thickness only has an effect on the forces when the skin depth is larger than the track thickness. Reducing the track thickness below the skin-depth increases the track resistance and predictably increases the thrust and decreased the lift force. A track thickness greater than 10mm would not be necessary because at high-speed the skin depth is at this level.

The conductivity has a very predictable effect on performance; a higher conductivity increases the lift force while decreasing the thrust, therefore using a lower conductivity track would improve the lift-to-weight ratio but decrease the thrust efficiency, the improvement in thrust efficiency between copper and aluminum conductivity was not significant compared to changes in pole number. Due to cost considerations, only a track constructed of aluminum was considered as feasible.

## 4 Methods to Further Improve the EDW Performance

There are a number of ways in which the thrust efficiency could be improved further. If higher strength magnet material could be used, or superconducting magnets were used, then the thrust efficiency could be improved further by increasing the number of poles while still providing a sufficient lift-to-weight ratio. The result of increasing the number of poles well beyond 10 pole-pairs is shown in Figure 20; at 100 pole-pairs the thrust efficiency reaches 87%.

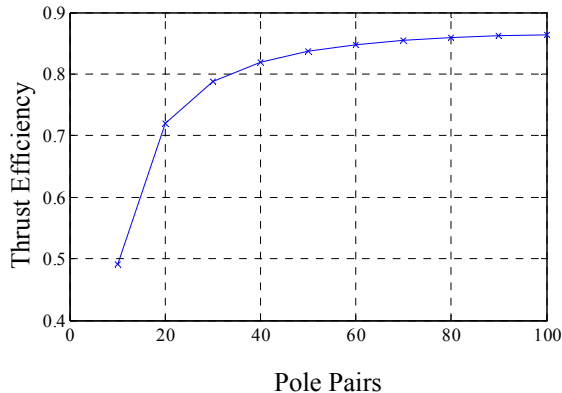


**Fig. 20. Thrust Efficiency vs. Pole Pairs**

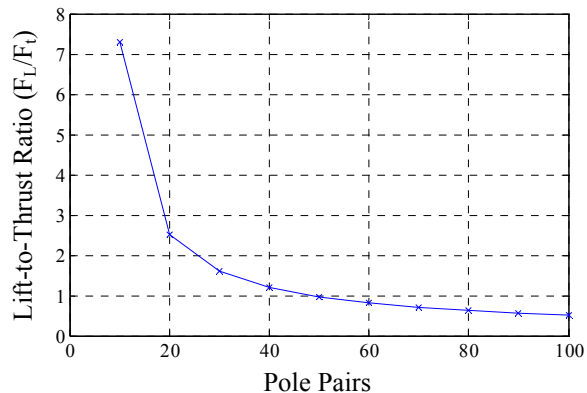


**Fig. 21. Lift-to-Thrust Ratio**

At such high pole numbers the magnitude of the lift force becomes less than the thrust force as shown in Figure 21 and therefore only at very high thrust would sufficient lift force be created.

A second method to improve performance is to use more than one EDW in series, and this would almost certainly be required for any large maglev vehicle. An illustration of a simulation with two EDW in series is shown in Figure 22. If the second EDW is close to the first then the currents induced in the track by the first EDW, can be used by the second, and thus less overall energy is required. The pertinent results from the simulation over the range of slip values for two EDW that are not interacting and two that are in close proximity, as in Figure 22, is shown in Figure 23 and 24. The force between the two interacting EDW becomes more complex. However, clearly there are slip values that result in improved thrust and lift efficiency.

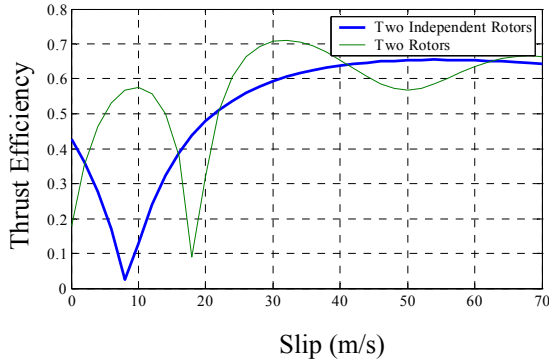


Fig. 23 Thrust Efficiency for two EDW's

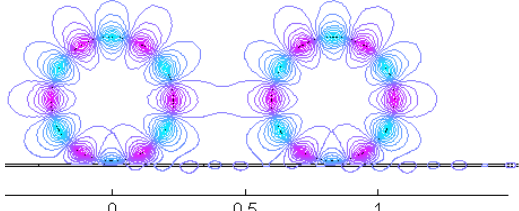


Fig. 22 Two EDW's in Series Separated by 0.4m

If the second EDW is close to the first then the currents induced in the track by the first EDW, can be used by the second, and thus less overall energy is required. The pertinent results from the simulation over the range of slip values for two EDW that are not interacting and two that are in close proximity, as in Figure 22, is shown in Figure 23 and 24. The force between the two interacting EDW becomes more complex. However, clearly there are slip values that result in improved thrust and lift efficiency.

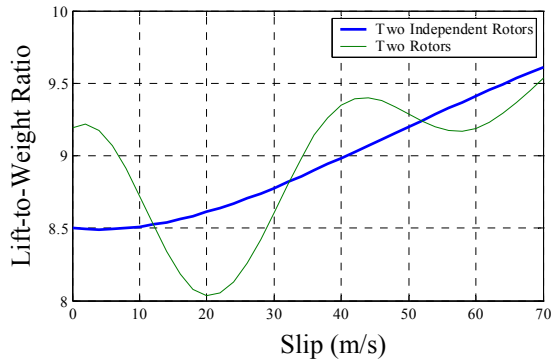


Fig. 24. Lift to Weight Ratio for two EDW's

Lastly, Post has suggested that levitation efficiency created by traditional linear motional electrodynamics can be improving significantly by increasing the inductance of the track, or reducing the skin effect losses by laminating the track or even using litz wire [7, 12]. These methods should also allow the thrust efficiency to be improved. However, such methods would increase the construction costs of a passive track structure.

## 5 Conclusion

A 2D parameter analysis of an EDW using Halbach magnets has been presented. Only the losses within the magnets were neglected. The results show that the pole number has the greatest influence on the performance of the EDW. Maximizing both the lift-to-weight ratio and thrust efficiency is limited by the maximum possible strength of the Halbach magnets. Greater improvements in performance could be achieved by using more than one EDW in series or reducing the skin effect losses, or increasing the track inductance. Although using a maglev vehicle driven by EDW's would require an onboard power source and further losses would be associated with mechanically rotating the EDW's, the very large savings in track construction costs makes this form of maglev enticing. Furthermore, the thrust efficiency achievable using the EDW approaches that which can be cost effectively attained using a linear synchronous motor. The thrust is attained by using the losses that occur due to the inherent drag force associated with almost all separate electromagnetic and electrodynamic levitation systems.

## 6 Acknowledgments

The authors would like to acknowledge the support provided by the member companies of the Wisconsin Electric Machines and Power Electronics Consortium (WEMPEC) at the University of

Wisconsin-Madison. Also, the authors would like to acknowledge the help provided by the Comsol Group (FEMLAB) and the Magsoft Corporation.

## 7 References

1. *Department of Transportation, Conceptual Design and Analysis of the Tracked Magnetically Levitated Vehicle Technology Program (TMLV) - Repulse Scheme, Vol. 1 Technical Studies.* 1975, FRA-OR&D-75-21.
2. Borcherts, R.H. and L.C. Davis, *The Superconducting Paddlewheel as an Integrated Propulsion Levitation Machine for High Speed Ground Transportation, Electric Machines and Electromechanics.* 1979: p. 341-355.
3. Davis, L.C. and R.H. Borcherts, *Superconducting Paddle Wheels, Screws, and other Propulsion Units for High-Speed Ground Transportation.* J. Appl. Phys., 1973. **44**(7): p. 3294-3299.
4. Bird, J. and T.A. Lipo, *An Electrodynamic Wheel: An Integrated Propulsion and Levitation Machine.* Electric Machines and Drives Conference, 2003. **3**: p. 1410-1416.
5. Fujii, N., G. Hayashi, and Y. Sakamoto, *Characteristics of magnetic lift, propulsion and guidance by using magnet wheels with rotating permanent magnets.* Industry Applications Conference, 2000: p. 257-262.
6. Fujii, N., O. Ogawa, and T. Matsumoto, *Revolving Magnet Wheels with Permanent Magnets.* Electrical Engineering in Japan, 1996. **116**(1): p. 106-117.
7. Post, R.F. and D.D. Ryutov, *The Inductrack: a simpler approach to magnetic levitation.* IEEE Trans. on Applied Superconductivity, 2000. **10**(1): p. 901 - 904.
8. Trumper, D.L., M.E. Williams, and T.H. Nguyen, *Magnet arrays for synchronous machines.* Industry Applications Society Annual Meeting, 1993. **1**: p. 9-18.
9. Boldea, I. and S.A. Nasar, *Linear Motion Electromagnetic Systems.* 1985: John Wiley & Sons. 461-478.
10. Hasebe, S. and Y. Kano, *Analysis of Three-Dimensional Magnetic Field Inducing Eddy Currents - on the Nature of Scalar Potential.* Electrical Engineering in Japan, 1983. **103**(6): p. 17-25.
11. Davey, K., *Optimization Shows Halbach Arrays to be Non-Ideal for Induction Devices.* IEEE Transactions on Magnetics, 2000. **36**(4): p. 1035-1038.
12. Post, R.F. and D.D. Ryutov, *The Inductrack Approach to Magnetic Levitation.* 2000, U.S. Department of Energy, UCRL-JC-138593.